Kinetic Studies with the Non-nucleoside HIV-1 Reverse Transcriptase Inhibitor U-88204E

Irene W. Althaus, James J. Chou,‡ Andrea J. Gonzales,§ Martin R. Deibel, Kuo-Chen Chou, Ferenc J. Kezdy, Donna L. Romero, John R. Palmer, Richard C. Thomas, Paul A. Aristoff, W. Gary Tarpley, and Fritz Reusser*

The Upjohn Company, Kalamazoo, Michigan 49001

Received February 9, 1993; Revised Manuscript Received April 5, 1993

ABSTRACT: The bis(heteroaryl)piperazine U-88204E is a potent inhibitor of HIV-1 reverse transcriptase (RT) and possesses excellent anti-HIV activity in HIV-1-infected lymphocytes grown in tissue culture. Enzymatic kinetic studies of the RNA- and DNA-dependent DNA polymerases of RT were carried out in order to determine whether the inhibitor interacts directly with the template:primer or deoxyribonucleotide triphosphate (dNTP) binding sites of the polymerase. The experimental results were analyzed using steady-state or Briggs–Haldane kinetics, by assuming that the template:primer binds to the enzyme first followed by the dNTP and that the polymerase functions processively. The results of the analysis show that the inhibitor acts as a mixed to noncompetitive inhibitor with respect to both the template:primer and the dNTP binding sites. The potency of U-88204E on the RNA-directed DNA polymerase activity depends on the base composition of the template:primer. The K_i values for the poly(rC):$(dG)_{10}$-directed reactions were at least 7 times lower than the ones for reactions directed by poly(rA):$(dT)_{10}$. The inhibitor did not inhibit the RNase H function of HIV-1 RT nor did it impair the RNA-directed DNA polymerase activity of HIV-2 RT. These data thus demonstrate the unique specificity of U-88204E for HIV-1 RT.

The RT enzyme is essential for the replication of the HIV virus and thereby presents a valid target to interdict the spread of the virus in the human host. RT-inhibiting nucleoside analogs such as AZT, ddI, and ddC have shown beneficial effects in AIDS patients. The relative toxicity and the development of strains resistant to these inhibitors justify the search and exploration for non-nucleoside RT inhibitors. Several classes of non-nucleoside inhibitors have been described recently. These include the dipyridodiazepinones (Merluzzi *et al.*, 1990; Wu *et al.*, 1991), the benzodiazepines or TIBO compounds (Pauwels *et al.*, 1990; Debyser *et al.*, 1991), the HEPT derivatives (Baba *et al.*, 1989, 1991), the pyridinones (Goldman *et al.*, 1991), polysulfates and polysulfonates (Mohan *et al.*, 1991; Gama Sosa *et al.*, 1991; De-Clercq, 1987; Baba *et al.*, 1988a,b, 1990; Anand *et al.*, 1990; Busso *et al.*, 1988; Moelling *et al.*, 1989; Schols *et al.*, 1988; Althaus *et al.*, 1992), and the bis(heteroaryl)piperazines (or BHAPs) (Romero *et al.*, 1991; Dueweke *et al.*, 1992; Althaus *et al.*, 1993).

The bis(heteroaryl)piperazine U-88204E (Figure 1) is a member of this last class of compounds and is a potent inhibitor of HIV-1 RT with excellent antiviral activity at nontoxic doses in HIV-1-infected lymphocytes grown in tissue culture (Romero *et al.*, 1991). The IC_{50} in the syncytia reduction assay, using HIV-1 IIIb infected MT-2 cells, was 0.3 μM U-88204E, and the IC_{50} in terms of cell toxicity was >27 μM. In the p24 release assay, carried out in HIV-1 (D34 isolate) infected peripheral blood mononuclear cells, the IC_{50} for the inhibition of p24 viral core protein released was 0.001 μM, and the IC_{50} in terms of cytotoxicity to the host cells was >10 μM. Moreover, U-88204E concentrations necessary to effectively inhibit normal cellular α and δ DNA polymerase activities were 1000–10000-fold higher than the ones required to inhibit RT. This report describes enzymatic kinetic studies, using recombinant HIV-1 RT, to examine the inhibitory effects of U-88204E on both the RNA- and DNA-dependent DNA polymerase functions of HIV-1 RT.

U-88204E

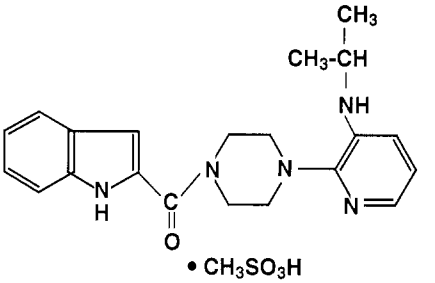

FIGURE 1: Chemical structure of U-88204E.

MATERIALS AND METHODS

The expression of HIV-1 RT and its purification have been described (Deibel *et al.*, 1990; Chattopadhyay *et al.*, 1992). The enzyme was devoid of *Escherichia coli* RNase H activity and consisted of p66/p51 heterodimers, as evidenced by gel electrophoresis.

The synthetic template:primers poly(rA):$(dT)_{10}$, poly(rC):$(dG)_{10}$, and poly(dC):$(dG)_{12-18}$ were purchased from Pharmacia. [α-^{35}S]-labeled dTTP and dGTP were purchased from Du Pont NEN. Nonidet P-40 was purchased from Sigma.

The standard reaction mixtures for the HIV-1 RT RNA-directed DNA polymerase assay contained 20 mM dithiothreitol, 60 mM NaCl, 0.05% Nonidet P-40, 10 mM $MgCl_2$, 50 mM Tris·HCl (pH 8.3), 10 μM of the cognate [α-^{35}S]-labeled deoxyribonucleotide 5′-triphosphate (final specific activity 1 Ci/mmol), 10 μg/mL RNA template [poly(rA) or

* Corresponding author. Phone: (616) 385-7152. FAX: (616) 385-7373. TELEX: 224401.

‡ Current address: Department of Physics, University of Michigan, Ann Arbor, MI 48109.

§ Current address: Curriculum for Toxicology, University of North Carolina, Chapel Hill, NC 27599.

0006-2960/93/0432-6548$04.00/0

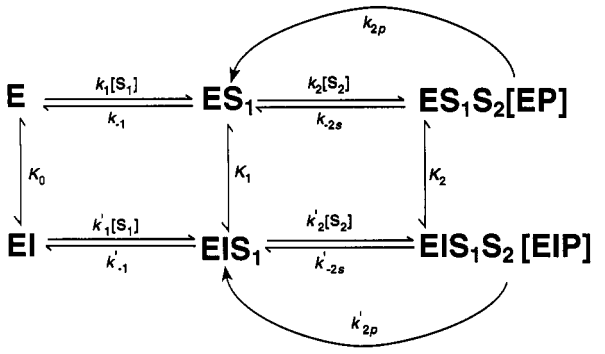

FIGURE 2: Steady-state reaction scheme for HIV RT: E = enzyme; S_1 = template:primer; S_2 = dNTP; K_0, K_1, K_2 = equilibrium constants between the inhibitor (I), the enzyme, and its substrates; EP = enzyme–product.

poly(rC)], 5 μg/mL of the appropriate primer [$(dT)_{10}$ or $(dG)_{10}$], and 0.16 μg of purified HIV RT. The total volume of the reaction mixtures was 50 μL. The samples were incubated at 37 °C for 15 min. The reactions were terminated by the addition of equal volumes of 10% trichloroacetic acid. Incorporation of radiolabeled precursor was determined by collecting the precipitates on glass fiber filters, drying, and counting the samples.

The DNA-directed DNA polymerase activity of the HIV-1 RT enzyme was assessed as described above for the RNA-directed DNA polymerase assay. The synthetic template:primer used was poly(dC):$(dG)_{12-18}$ (1:1), present at a concentration of 10 μg/mL.

The HIV-1 RNase H assay was conducted as described (Tan *et al.*, 1991). In general, the assay follows the loss of a trichloroacetic acid precipitatable radiolabeled RNA:DNA hybrid as a function of time. The specific assay mixtures contained 1.25 μg/mL [^{3}H]poly(rA):poly(dT) (1:1), 50 mM Tris·HCl (pH 8.5), 5 mM $MgCl_2$, 0.02% Nonidet P-40, 3% glycerol, 0.1 mg/mL BSA, and 0.05 μg of enzyme. Sample aliquots were removed and spotted on glass fiber papers, which where immediately immersed in 5% cold trichloroacetic acid. Reaction velocities were determined by the decrease in radioactivity as a function of time.

The HIV-2 RNA-directed DNA polymerase assay was carried out as described above for the corresponding assay system with HIV-1 RT. The template:primer used was poly-(rA):$(dT)_{10}$. Sufficient enzyme was added per reaction mixture to incorporate approximately 0.04 nmol of dTMP in 15 min at 37 °C.

The kinetic experiments were run in duplicate and confirmed in at least three or more separate experiments. The kinetic data were initially analyzed using Michaelis–Menten kinetics, which is based on a rapid equilibrium system. This analysis yielded contradictory results in some cases. The rapid equilibrium treatment was thus abandoned, and the data were analyzed using steady-state or Briggs–Haldane kinetics. In this latter case, the enzyme–substrate complex does not need to be in equilibrium with the enzyme and its substrate. However, shortly after initiation of the reaction, the enzyme–substrate complex is formed at the same rate at which it dissociates. Steady-state schemes including all of the reaction steps to be considered here yield very complex velocity equations which are impractical to solve. For these reasons, the general steady-state kinetic system used in this study was simplified as detailed in Figure 2. The specific rate constants used in the following paragraph are defined in this figure.

The steady-state kinetics was limited to the reactions occurring between the enzyme and the substrates, while rapid equilibrium kinetics was applied to the processes pertaining to the inhibitor-releasing or inhibitor-binding reactions by the enzyme or the various enzyme–substrate complexes. Moreover, an ordered mechanism was assumed, whereby the template:primer complex binds first to the enzyme followed by the addition of dNTP (Majumbdar *et al.*, 1988; Reardon, 1992). The polymerase is a processive enzyme, and after the addition of the first nucleotide, translocation occurs along the template, resulting in the incorporation of further nucleotides into the growing chain (Majumbdar *et al.*, 1988). Under these conditions the formation of the phosphoester bond can be considered to be irreversible as the reverse reaction occurs at an extremely low rate. In addition, the dissociation of the enzyme–product complex into its components is also negligible during the initial reaction phase. Thus, the enzyme–product does not differ from the initial enzyme–template:primer complex in that the former shuttles back to the enzyme–template:primer state and this reaction rate constant (k_{2p}) is equal to k_{cat}, representing the turnover number. The quaternary enzyme–inhibitor–template:primer–dNTP complex should be nonproductive as no translocation to the enzyme–inhibitor–template:primer state should occur and k'_{2p} would be 0. These simplifications reduce the number of parameters to be considered in the system to 12 or 13 if we include k'_{2p}.

The HIV RT-catalyzed system considered here consists of two substrates, S_1, representing the template:primers, and S_2, representing the dNTP, and an inhibitor. The reactions between the enzyme (E) and the low molecular weight inhibitor (I) can be deemed diffusion-controlled reactions (Chou & Jiang, 1974; Chou, 1976; Chou & Zhou, 1982). Consequently, the conversions between E and EI, ES_1 and EIS_1, and ES_1S_2 and EIS_1S_2 occur at a much faster rate than the interconversions between the enzyme and its substrates. Thus, although the whole system is a steady-state one, there is an equilibrium between the inhibitor and the enzyme and the enzyme–substrate complexes (Cha, 1968). Accordingly, the kinetic relations between E and EI, ES_1 and EIS_1, and ES_1S_2 and EIS_1S_2 can be expressed in terms of the equilibrium constants K_0, K_1, and K_2, respectively, as defined below:

$$K_0 = \frac{[E][I]}{[EI]} \quad K_1 = \frac{[ES_1][I]}{[EIS_1]} \quad K_2 = \frac{[ES_1S_2][I]}{[EIS_1S_2]} \tag{1}$$

Using the apparent rate constants method (Cha, 1968), the mechanism expressed in Figure 2 can be further reduced to the one shown in Figure 3 (see the Appendix). According to Chou's graphic rules (see the Appendix), the mechanism in Figure 3 can be expressed by a directed graph G (Figure 4a) and the transformed graph $G^\dagger$ (Figure 4b), where E_1 = E + EI, E_2 = ES_1 + EIS_1, E_3 = ES_1S_2 + EIS_1S_2 and

$$\begin{cases} k_{12} = \dfrac{(k_{+1}K_0 + k'_{+1}[I])[S_1]}{K_0 + [I]} \\ k_{21} = \dfrac{k_{-1}K_1 + k'_{-1}[I]}{K_1 + [I]} \\ k_{23} = \dfrac{(k_{+2}K_1 + k'_{+2}[I])[S_2]}{K_1 + [I]} \\ k_{32} = \dfrac{(k_{-2s} + k_{+2p})K_2 + (k'_{-2s} + k'_{+2p})[I]}{K_2 + [I]} \end{cases} \tag{2}$$

Thus, the concentration of the mth enzyme species is given

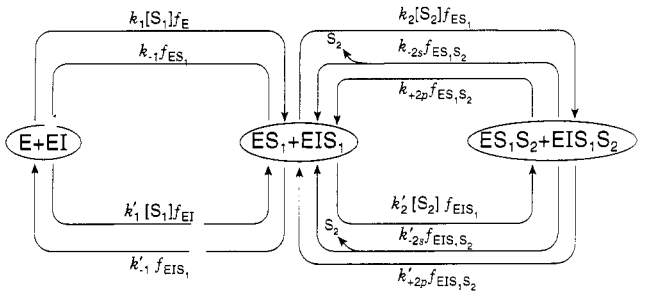

FIGURE 3: Enzyme-catalyzed mechanism derived from Figure 2 by means of the apparent rate constant method (Cha, 1968).

by (see the Appendix)

$$[E_m] = \frac{N_m}{\sum_{i=1}^{n} N_i} e_0 \qquad (m = 1, 2, ..., n) \tag{3}$$

where e_0 is the total concentration of all enzyme species and

$$\begin{cases} N_1 = k_{32}k_{21} \\ N_2 = k_{12}k_{32} \\ N_3 = k_{12}k_{23} \end{cases} \tag{4}$$

Substitution of eq 4 into eq 3 yields

$$[E_3] = \frac{k_{12}k_{23}e_0}{k_{32}k_{21} + k_{12}k_{32} + k_{12}k_{23}} \tag{5}$$

Thus, the rate of product formation is

$$\frac{d[P]}{dt} = \frac{k_{12}k_{23}(k_{+2p}K_2 + k'_{+2p}[I])/(K_2 + [I])}{k_{32}k_{21} + k_{12}k_{32} + k_{12}k_{23}} e_0 \tag{6}$$

RESULTS

RNA-Dependent DNA Polymerase. In one set of experiments, this function was studied in the presence of varied concentrations of poly(rA):$(dT)_{10}$ and a fixed concentration of dTTP and vice versa in the presence of varied concentrations of dTTP and a fixed concentration of poly(rA):$(dT)_{10}$. Three inhibitor concentrations were used in addition to controls containing no U-88204E. The analysis of the kinetic data was carried out via computer using the steady-state kinetic scheme described in Materials and Methods. The experimental results are shown in Table I, and the calculated essential forward and backward reaction rates and equilibrium constants of the system are given in Figure 5. The calculated rate constants derived by fitting the experimental data to eq 6 for k_1, representing the association constant, and k_{-1}, representing the dissociation rate constant of the enzyme–poly(rA):$(dT)_{10}$ complex, were 4.4×10^4 M^{-1} s^{-1} and 0.34 s^{-1}, respectively, in the absence of the inhibitor. In the presence of U-88204E, the corresponding values were 3.4×10^4 M^{-1} s^{-1} for k'_1 and 0.28 s^{-1} for k'_{-1}. The forward rate constant k_2 for the association of dTTP to its cognate enzyme–template:primer complex was 3.4×10^4 M^{-1} s^{-1}. The backward rate constant k_{-2s}, representing the dissociation rate of the enzyme–template:primer–dTTP complex, was 0.87 s^{-1}. The corresponding values in the presence of inhibitor were $k'_2 = 0.7 \times 10^4$ M^{-1} s^{-1} and $k'_{-2s} = 0.87$ s^{-1}. The turnover number k_{2p}, representing k_{cat}, was 0.9 s^{-1} in the control reaction, and the corresponding value k'_{2p} in the presence of the inhibitor was essentially 0. The value for k_{2p} is somewhat lower than the one reported by Reardon (1992) (14 s^{-1}) but in good agreement with the one reported by Anderson and Coleman (1992) (1.2 s^{-1}), although both of the latter values were calculated with different mathematical schemes than the one applied here. Moreover, the respective inhibition constants or K_i's calculated for the

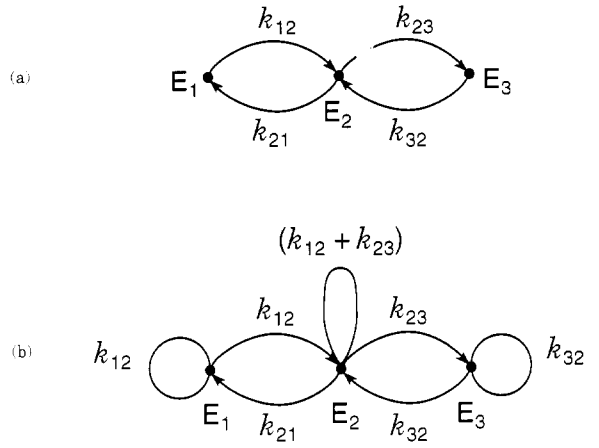

FIGURE 4: Graphical expression of the mechanism shown in Figure 3: (a) digraph G; (b) a's transformed graph $G^\dagger$ (Chou, 1989, 1990). $E_1 = E + EI$, $E_2 = ES_1 + EIS_1$, and $E_3 = ES_1S_2 + EIS_1S_2$, and k_{12}, k_{21}, k_{23}, and k_{32} are given by eq 2.

Table I: Inhibition of HIV-1 RT Poly(rA):$(dT)_{10}$-Directed Poly(dT) Synthesis by U-88204E[a]

U-88204E (μM)	poly(rA):$(dT)_{10}$ (μM)	dTTP (μM)	d[P]/dt (μM × 10^{-6} s^{-1})
0	0.75	152	3301
2	0.75	152	3062
4	0.75	152	2331
6	0.75	152	2104
0	1.50	152	5896
2	1.50	152	4838
4	1.50	152	3565
6	1.50	152	2583
0	3.00	152	8026
2	3.00	152	6489
4	3.00	152	4775
6	3.0	152	3477
0	4.50	152	10911
2	4.50	152	7900
4	4.50	152	5216
6	4.50	152	3666
0	7.5	3.8	1947
2	7.5	3.8	1312
4	7.5	3.8	972
6	7.5	3.8	719
0	7.5	7.6	3470
2	7.5	7.6	2222
4	7.5	7.6	1417
6	7.5	7.6	1142
0	7.5	15.2	7492
2	7.5	15.2	4465
4	7.5	15.2	2814
6	7.5	15.2	2116
0	7.5	38	11387
2	7.5	38	5969
4	7.5	38	4211
6	7.5	38	3175

[a] Enzyme = 0.0274 μM; d[P]/dt = μM × 10^{-6} dTMP incorporated per second.

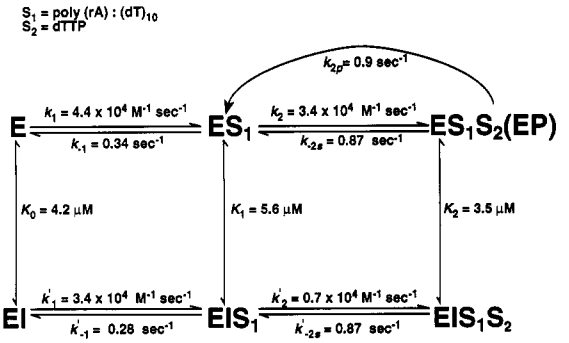

FIGURE 5: Inhibition of poly(rA):$(dT)_{10}$-directed poly(dT) synthesis by U-88204E; steady-state kinetic parameters.

enzyme (K_0), the enzyme–template:primer (K_1), and the enzyme–template:primer–dTTP (K_2) complexes with the inhibitor were 4.2, 5.6, and 3.5 μM U-88204E. The overall fitting error for the analysis was 9×10^{-5}. The low value for k_{-1}, amounting to 0.34 s^{-1}, is indicative of a processive enzyme, and the results are consistent with an ordered mechanism whereby the template:primer binds to the enzyme first, followed by the addition of dNTP. The values for the equilibrium constants (K_0, K_1, and K_2) assessing the reactions between the inhibitor and the enzyme or the enzyme–substrate complexes are of the same magnitude. This suggests that U-88204E acts mainly as a noncompetitive inhibitor with respect to either the poly(rA):$(dT)_{10}$ or dTTP binding sites.

Similar experiments were carried out with the homopolymeric template:primer poly(rC):$(dG)_{10}$ and the cognant nucleotide dGTP. The experimental results are given in Table II, and the calculated values for the rate and equilibrium constants are shown in Figure 6. The forward rate constant, k_1, for the formation of the enzyme–template:primer complex was 5×10^4 M^{-1} s^{-1}, and the corresponding backward rate, k_{-1} was 0.39 s^{-1}. In the presence of the inhibitor, the forward reaction rate, k'_1, for the formation of the enzyme–U-88204E–poly(rC):$(dG)_{10}$ complex was 3.3×10^4 M^{-1} s^{-1}, and the value for k'_{-1}, the reverse reaction, was 0.18 s^{-1}. Moreover, the forward reaction rate for the formation of the ternary enzyme–template:primer–dGTP complex, k_2, was 2×10^4 M^{-1} s^{-1} and the backward rate, k_{-2s}, was 0.89 s^{-1}. In the presence of the inhibitor, k'_2, the rate of formation of the quaternary enzyme–U-88204E–template:primer–dGTP complex was 0.64×10^4 M^{-1} s^{-1}, and the corresponding dissociation rate, k'_{-2s}, for this complex was 0.9 s^{-1}. The turnover number or rate of translocation (k_{2p}) was 1 s^{-1} in the absence of the inhibitor, and the corresponding value, k'_{2p}, for the quaternary enzyme–U-88204E–template:primer–dGTP complex was essentially 0. The dissociation constant K_0 was 4.3 μM U-88204E for the enzyme–inhibitor complex, the value was 0.5 μM for K_1 (the enzyme–inhibitor–template:primer complex), and the value was 0.25 μM for K_2 (the enzyme–inhibitor–template:primer–dGTP complex). The fitting error was 1×10^{-5} for this system. The value for K_0 is higher than the ones for K_1 and K_2 and shows that U-88204E binds more tightly to the enzyme–substrate complexes than the free enzyme. The compound thus acts as a mixed inhibitor with respect to the poly(rC):$(dG)_{10}$ and dGTP binding sites. These K_1 and K_2 values are approximately 10 times smaller than the corresponding ones obtained with the poly(rA):$(dT)_{10}$-catalyzed systems, and they show that the potency of U-88204E is somewhat dependent on the base composition of the template:primer.

DNA-Directed DNA Polymerase of HIV-1 RT. U-88204E was also tested for its effect on the DNA-directed DNA polymerase activity of RT with poly(dC):$(dG)_{12-18}$ as the template:primer and dGTP as the nucleotide. The inhibitor was studied in the presence of varying amounts of poly(dC):$(dG)_{12-18}$ and a fixed amount of dGTP and vice versa. The experimental results are listed in Table III, and the calculated rate constants are in Figure 7. In the absence of the inhibitor, the value for k_1 was 6.3×10^4 M^{-1} s^{-1} and the one for k_{-1} was 0.2 s^{-1}, representing the respective forward and backward reaction rates for the formation and dissociation of the enzyme–poly(dC):$(dG)_{12-18}$ complex. In the presence of the inhibitor, the corresponding forward and backward reaction rates were $k'_1 = 3.9 \times 10^4$ M^{-1} s^{-1} and $k'_{-1} = 0.2$ s^{-1}. The forward reaction rate for the formation of the enzyme–poly(dC):$(dG)_{12-18}$–dGTP complex, k_2, was 7.4×10^4 M^{-1} s^{-1}, and the corresponding backward rate constant, k_{-2s}, was 0.8 s^{-1}. In the presence of the inhibitor, k'_2 was 0.8×10^4 M^{-1} s^{-1} and k'_{-2s} was 0.5 s^{-1}. The turnover number k_{2p} was 0.9

Table II: Inhibition of HIV-1 RT Poly(rC):$(dG)_{10}$-Directed Poly(dT) Synthesis by U-88204E[a]

U-88204E (μM)	poly(rC):$(dG)_{10}$ (μM)	dGTP (μM)	d[P]/dt (μM × 10^{-6} s^{-1})
0.0	0.45	72.0	797
0.25	0.45	72.0	630
0.5	0.45	72.0	488
1.0	0.45	72.0	345
0.0	0.75	72.0	1261
0.25	0.75	72.0	1011
0.5	0.75	72.0	785
1.0	0.75	72.0	535
0.0	1.50	72.0	1690
0.25	1.50	72.0	1451
0.5	1.50	72.0	1095
1.0	1.50	72.0	750
0.0	3.00	72.0	2582
0.25	3.00	72.0	2120
0.5	3.00	72.0	1690
1.0	3.00	72.0	1071
0.0	7.5	3.6	1608
0.25	7.5	3.6	1034
0.5	7.5	3.6	757
1.0	7.5	3.6	412
0.0	7.5	7.2	2501
0.25	7.5	7.2	1530
0.5	7.5	7.2	1197
1.0	7.5	7.2	718
0.0	7.5	14.4	2994
0.25	7.5	14.4	1769
0.5	7.5	14.4	1344
1.0	7.5	14.4	825
0.0	7.5	21.6	3446
0.25	7.5	21.6	2248
0.5	7.5	21.6	1477
1.0	7.5	21.6	891

[a] Enzyme = 0.0274 μM; d[P]dt = μM × 10^{-6} dGMP incorporated per second.

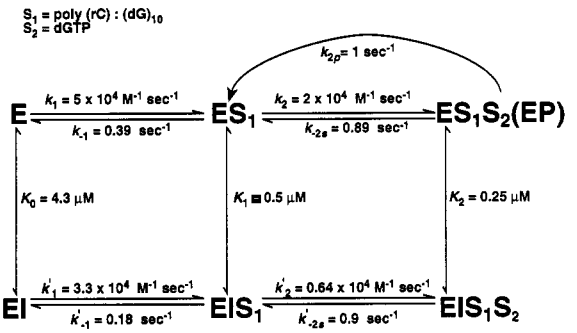

FIGURE 6: Inhibition of poly(rC):$(dG)_{10}$-directed poly(dG) synthesis by U-88204E; steady-state kinetic parameters.

Table III: Inhibition of HIV-1 RT Poly(dC):$(dG)_{12-18}$-Directed Poly(dG) Synthesis by U-88204E[a]

U-88204E (μM)	poly(dC):$(dG)_{12-18}$ (μM)	dGTP (M)	d[P]/dt (μM × 10^{-6} s^{-1})
0	0.2	300	7235
10	0.2	300	4985
15	0.2	300	4771
20	0.2	300	4292
0	0.4	300	12006
10	0.4	300	7211
15	0.4	300	6678
20	0.4	300	6193
0	0.5	300	14948
10	0.5	300	8348
15	0.5	300	7704
20	0.5	300	7235
0	0.75	300	16515
10	0.75	300	9542
15	0.75	300	8619
20	0.75	300	7944
0	1.0	300	19243
10	1.0	300	10884
15	1.0	300	9382
20	1.0	300	8873
0	10.0	3.7	2126
2	10.0	3.7	1930
4	10.0	3.7	1594
8	10.0	3.7	1013
0	10.0	7.5	4034
2	10.0	7.5	3434
4	10.0	7.5	2931
8	10.0	7.5	1698
0	10.0	15	6897
2	10.0	15	4641
4	10.0	15	3334
8	10.0	15	2136
0	10.0	22.5	10557
2	10.0	22.5	6021
4	10.0	22.5	4183
8	10.0	22.5	2619

[a] Enzyme = 0.0274 μM; d[P]/dt = μM × 10^{-6} dGMP incorporated per second.

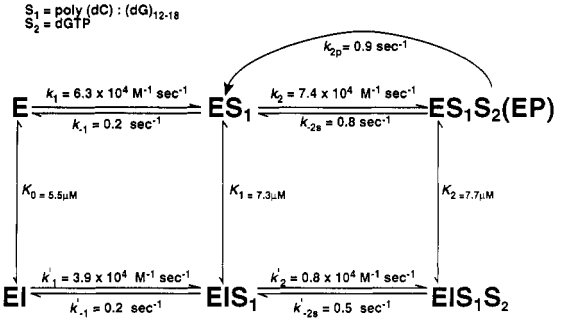

FIGURE 7: Inhibition of poly(dC):$(dG)_{12-18}$-directed poly(dG) synthesis by U-88204E; steady-state kinetic parameters.

s^{-1} for the control reaction and essentially 0 for k'_{2p} in this system. The dissociation constants for the inhibitor complexes were K_0 = 5.5, K_1 = 7.3, and K_2 = 7.7 μM U-88204E, respectively. The fitting error was 1.9 × 10^{-4} for this system. Since the K_i constants are nearly equal, the inhibitor acts as a noncompetitive inhibitor with respect to the poly(dC):$(dG)_{12-18}$ and dGTP binding sites of the DNA-directed DNA polymerase domain of HIV RT.

RNase H Assay. U-88204E was also tested for inhibitory activity against the RNase H function of HIV-1 RT. The substrate was a full-length poly(rC):(dG) homopolymeric hybrid, with the RNA component being labeled with ^3H. The compound did not impair the RNase H function of HIV-1 RT when tested at concentrations of up to 100 μM.

HIV-2 RT. The compound did not inhibit the RNA-dependent DNA polymerase activity of this enzyme when tested at concentrations of up to 100 μM.

DISCUSSION

The inhibition kinetics of U-88204E on the RNA- and DNA-directed DNA polymerase domains of HIV-1 RT were studied with respect to the nucleic acid and dNTP binding sites using homopolymeric template:primers. The analysis of the experimental results were carried out using a modified steady-state or Briggs–Haldane kinetic scheme. These kinetics take into consideration the following observations: (a) The reaction is ordered in that the template:primer binds first to the enzyme and is followed by the addition of dNTP. (b) The enzyme–product complex elongated by one base does not dissociate into free enzyme and product but is recycled back to the enzyme–template:primer state by the process of translocation, and the polymerase is, therefore, processive. (c) The formation of the phosphoester bond and the concomitant release of pyrophosphate is irreversible, as the reverse reaction rate is extremely slow. (d) The binding of the low molecular weight inhibitor to the free enzyme or the various enzyme–substrate complexes follows rapid equilibrium kinetics. (e) The enzyme–inhibitor–template:primer–dNTP complex is nonproductive and k'_{2p} = 0.

The rate equation derived for this mechanism contains 12 rate constants as defined in Figure 2. These include the equilibrium constants or K_i's, defined as K_0, K_1, and K_2, assessing the reactions between the inhibitor and the enzyme and the various enzyme–inhibitor complexes. The values calculated for these constants are indicative of the type of inhibitor under study, e.g., competitive, noncompetitive, mixed, or uncompetitive. If K_0 yields a finite solution and K_1 and K_2 are infinite, then the inhibitor is a competitive inhibitor with respect to the template:primer as it competes with this substrate for its binding site. Similarly, if both values for K_0 and K_1 are finite and K_2 is infinite, the inhibitor competes with the dNTP binding site and is a competitive inhibitor with respect to this latter site. Conversely, if K_0 and K_1 are infinite and K_2 is finite or K_0 is infinite and K_1 and K_2 are finite, the inhibitor acts uncompetitively, meaning that it binds only to the enzyme–template:primer–dNTP complex or the enzyme–template:primer complex, but not to the free enzyme. If all three K_i values are finite and equal in value, the inhibitor acts as a pure noncompetitive inhibitor with respect to both substrate binding sites on the RT; in the event that the three K_i's are finite but deviate significantly from each other, the compound acts as a mixed inhibitor.

The velocity eq 6 allows the calculation of the essential rate constants and relates the amount of product formed by the RT enzyme to the two substrates, the template:primer, and the dNTP. The calculated dissociation constants for the enzyme–template:primer (k_{-1}) complexes in the absence of inhibitor ranged around 0.2–0.34 s^{-1} in both the RNA- and DNA-catalyzed DNA polymerase reactions studied. These values are very small and are characteristic of processive polymerases. The turnover numbers k_{2p} (or k_{cat}) for the RNA- and DNA-directed polymerase functions were approximately 1 s^{-1} and are somewhat smaller than a previously published value of 14 s^{-1} for HIV-1 RT (Reardon, 1992), but are in good agreement with a value of 1.2 s^{-1} published by Anderson and Coleman (1992). The equilibrium constants K_1 and K_2 for the enzyme–substrate–inhibitor complexes were approximately 10 times larger in the poly(rA):$(dT)_{10}$-catalyzed reactions than the ones obtained with the poly(rC):$(dG)_{10}$-directed reactions, which shows that the potency of U-88204E

is somewhat dependent on the base composition of the template:primer. The values for K_1 and K_2 (7.3 and 7.7 μM) calculated for the DNA-directed DNA polymerase were higher than the ones obtained for the poly(rC):$(dG)_{12-18}$-catalyzed RNA-directed DNA polymerase. Moreover, the equilibrium constants (K_0, K_1, and K_2) for the enzyme–inhibitor (EI), the enzyme–template:primer–inhibitor (EIS_1), and the enzyme–template:primer–dNTP–inhibitor (EIS_1S_2) complexes were nearly equal for the poly(rA):$(dT)_{10}$- and poly(dC):$(dG)_{12-18}$-directed systems. This indicates that U-88204E acts as a noncompetitive inhibitor with respect to these template:primer and nucleotide binding sites of the RT enzyme. In the case of the poly(rC):$(dG)_{10}$-catalyzed reactions, the K_1 and K_2 values are significantly smaller than the one for K_0, which is indicative of a mixed inhibitor.

HIV-2 RT was insensitive to U-88204E, demonstrating the unique sensitivity of HIV-1 RT to this inhibitor. In a previous communication (Althaus *et al.*, 1993), we described the inhibition kinetics of U-87201E, a compound structurally related to U-88204E. Both compounds inhibit the RNA- and DNA-directed DNA polymerase functions of RT but not the RNase H activity; however, U-87201E acts mainly as a noncompetitive inhibitor while U-88204E acts as a mixed to noncompetitive inhibitor with respect to the template:primer and dNTP binding sites of the RT enzyme. U-88204E also differs from U-87201E in that the former is considerably more potent than the latter in all of the systems tested, which indicates that U-88204E binds much tighter to the free enzyme and the various enzyme–substrate complexes than U-87201E. Moreover, the potency of U-88204E depends on the base composition of the homopolymeric template:primers studied; the potency of U-87201E is independent of the base composition of the polymers.

Recently, kinetic studies with other non-nucleoside HIV-1 RT inhibitors have been described using Michalis–Menten kinetics. The benzodiazepine or TIBO compound R82150 appears to be a specific inhibitor of the HIV-1 RT-catalyzed RNA-directed DNA polymerase function (Debyser *et al.*, 1991). The inhibitor acts uncompetitively with respect to the nucleic acid binding site and noncompetitively with respect to the dNTP site. The IC_{50} for the DNA-directed DNA polymerase was 40 times higher than the one required to inhibit the RNA-directed DNA polymerase, and the RNase H activity was not impaired by the inhibitor. The dipyridodiazepinone nevirapine acts as a mixed inhibitor with respect to the poly(rA):$(dT)_{10}$ and poly(rC):$(dG)_{10}$ binding sites, and it acts noncompetitively with respect to the dNTP binding sites during RNA-directed DNA synthesis by HIV-1 RT (Tramontano & Cheng, 1992). The pyridinone derivative L-697,639 indicated noncompetitive inhibition with respect to dGTP and poly(rC):$(dG)_{12-18}$ (Goldman *et al.*, 1991). Compared with these other classes of RT inhibitors, some of the inhibition patterns of U-88204E are shared with the ones of the TIBO compound R82150, nevirapine, and the pyridinone L-697,639 discussed above. All are specific inhibitors of HIV-1 RT, they do not inhibit the RNase H function of HIV-1 RT, and they act noncompetitively with respect to the dNTP binding site of the RNA-directed DNA polymerase. With respect to the nucleic acid binding site, studied with synthetic RNA:DNA homopolymers, their properties diverge somewhat in that L-697,639 acts as a noncompetitive inhibitor, the TIBO compound R82150 acts mainly as an uncompetitive inhibitor, nevirapine acts as a mixed inhibitor, and U-88204E acts as a mixed to noncompetitive inhibitor. It should be emphasized, however, that all of these data, except for those obtained with the bis(heteroaryl)piperazines U-87201E (Althaus *et al.*, 1993) and U-88204E presented in this article, were analyzed using Michaelis–Menten kinetics and not steady-state kinetics.

ACKNOWLEDGMENT

We thank R. S. Goody of the Max Planck Institute, Heidelberg, Germany, for his generous gift of HIV-2 reverse transcriptase. We also thank Ms. Joan V. Vroegop for her assistance in drawing Figures 3 and 4 and Mrs. Jan K. Zelenock for editing the text.

APPENDIX

Derivation of Figures 3 and 4 and Equations 2–5. Here let us provide the detailed procedures of how to use the apparent rate constant method (Cha, 1968) and Chou's graphical rules (Chou, 1989, 1990; Lin & Neet, 1990) to simplify the mechanism of Figure 2 and derive eqs 2–4.

Since, in the steady-state system depicted in Figure 2, there is a rapid equilibrium between E and EI, ES_1 and EIS_1, and ES_1S_2 and EIS_2S_2, these three pairs of enzyme species can be, respectively, treated as three combined enzyme species, E+EI, ES_1+EIS_1, and ES_1S_2+EIS_1S_2, in which, however, the fractions of E, EI, ES_1, EIS_1, ES_1S_2, and EIS_1S_2 are given as

$$\begin{cases} f_E = \dfrac{[E]}{[E]+[EI]} = \dfrac{K_0}{K_0+[I]} \\ f_{EI} = \dfrac{[EI]}{[E]+[EI]} = \dfrac{[I]}{K_0+[I]} \\ f_{ES_1} = \dfrac{[ES_1]}{[ES_1]+[EIS_1]} = \dfrac{K_1}{K_1+[I]} \\ f_{EIS_1} = \dfrac{[EIS_1]}{[ES_1]+[EIS_1]} = \dfrac{[I]}{K_1+[I]} \\ f_{ES_1S_2} = \dfrac{[ES_1S_2]}{[ES_1S_2]+[EIS_1S_2]} = \dfrac{K_2}{K_2+[I]} \\ f_{EIS_1S_2} = \dfrac{[EIS_1S_2]}{[ES_1S_2]+[EIS_1S_2]} = \dfrac{[I]}{K_2+[I]} \end{cases} \quad \text{(A.1)}$$

where the equilibrium constants K_0, K_1, and K_2 are defined in eq 1. Thus, instead of the mechanism depicted in Figure 2, which contains six enzyme species, we can consider a simplified mechanism in which there are only three independent enzyme species, as shown in Figure 3. In doing so, however, the corresponding rate constants should be modified by multiplying them by a fractional factor (Cha, 1968). For the case considered here, the rate constant associated with E should be multiplied by f_E, that associated with EI by f_{EI}, that associated with ES_1 by f_{ES_1}, and so forth, as shown in Figure 3.

According to Chou's graphic rule 2, "if there are two or more arcs from one enzyme species to another, i.e. the so-called 'parallel pathways', then condense them into one by adding their rate constants together" (Chou, 1989, 1990). Thus, Figure 3 can be further simplified to Figure 4a, the socalled directed graph, G, where

$$\begin{cases} k_{12} = k_1[S_1]f_E + k'_1[S_1]f_{EI} \\ k_{21} = k_{-1}f_{ES_1} + k'_{-1}f_{EIS_1} \\ k_{23} = k_2[S_2]f_{ES_1} + k'_2[S_2]f_{EIS_1} \\ k_{32} = k_{-2s}f_{ES_1S_2} + k_{+2p}f_{ES_1S_2} + k'_{-2s}f_{EIS_1S_2} + k'_{+2p}f_{EIS_1S_2} \end{cases} \quad \text{(A.2)}$$

Substitution of the fractional factors of eq A.1 into eq A.2 yields eq 2 in the text.

Moreover, to each point in Figure 4a "add a loop with a weight equal to the sum of weights of the arcs departing from that point" (Chou, 1989, 1990), and then the graph G of Figure 4a is transformed to graph $G^{\dagger}$ of Figure 4b. Thus, according to Chou's graphic rule 2, the concentration of the mth (m = 1, 2, ..., n) enzyme species is given by eq 3, in which N_m can be derived directly from graph $G^{\dagger}$. The procedure is as follows: "For any selected reference point, e.g., E_r, in $G^{\dagger}$, find all those subgraphs each of which must contain one, and only one, path from E, to E_m, as well as all cycles and loops that intersect with neither each other nor the path; then for each subgraph, take the product of all its weights..." (Chou, 1989, 1990). For example, in calculating N_1, if E_3 is selected as a reference point, then we immediately obtain the first expression of eq 4. Again, in order to calculate N_2 and N_3, if E_1 is selected as a reference point, then we obtain the second and third expressions of eq 4. Substituting eq 4 into eq 3, we obtain eq 5. The merit of using the graphic rule is that the more complicated the system, the more efficient the derivation. The Chou graphic rules can also be used to analyze non-steady-state enzyme-catalyzed systems [see, for example, Lin and Neet (1990)].

REFERENCES

Althaus, I. W., LeMay, R. J., Gonzales, A. J., Deibel, M. R., Sharma, S. K., Kezdy, F. J., Resnick, L., Busso, M. E., Aristoff, P. A., & Reusser, F. (1992) *Experientia 48*, 1127–1132.

Althaus, I. W., Chou, J. J., Gonzales, A. J., Deibel, M. R., Chou, K. C., Kezdy, F. J., Romero, D. L., Aristoff, P. A., Tarpley, W. G., & Reusser, F. (1993) *J. Biol. Chem. 268*, 6119–6124.

Anand, R., Nayyar, S., Galvin, T. A., Merril, C. R., & Bigelow, L. B. (1990) *AIDS Res. Human Retroviruses 6*, 679–689.

Anderson, S. F., & Coleman, J. E. (1992) *Biochemistry 31*, 8221–8228.

Baba, M., Snoek, R., Pauwels, R., & De-Clercq, E. (1988a) *Antimicrob. Agents Chemother. 32*, 1742–1745.

Baba, M., Nakajima, M., Schols, D., Pauwels, R., Balzarini, J., & De-Clercq, E. (1988b) *Antiviral Res. 9*, 335–343.

Baba, M., Tanaka, H., De-Clercq, E., Pauwels, R., Balzarini, J., Schols, D., Nakashima, H., Perno, C. F., Walker, R. T., & Miyasaka, T. (1989) *Biochem. Biophys. Res. Commun. 165*, 1375–1381.

Baba, M., Schols, D., Pauwels, R., Nakashima, H., & De-Clercq, E. (1990) *J. Acquired Immune Defic. Syndr. 3*, 493–499.

Baba, M., De-Clercq, E., Tanaka, H., Ubasawa, M., Takashima, H., Sekiya, K., Nitta, I., Umezu, K., Nakashima, H., Mori, S., Shigeta, S., Walker, R. T., & Miyasaka, T. (1991) *Proc. Natl. Acad. Sci. U.S.A. 88*, 2356–2360.

Busso, M. E., Mian, A. M., Hahn, E. F., & Resnick, L. (1988) *AIDS Res. Human Retroviruses 4*, 449–455.

Cha, S. (1968) *J. Biol. Chem. 35*, 820–825.

Chattopadhyay, D., Einspahr, H. M., Brunner, D. P., Strakalaitis, N. A., Tarpley, W. G., & Deibel, M. R. (1992) *Protein Expression Purif. 3*, 151–159.

Chou, K. C. (1976) *Sci. Sin. 19*, 505–528.

Chou, K. C. (1989) *J. Biol. Chem. 264*, 12074–12079.

Chou, K. C. (1990) *Biophys. Chem. 35*, 1–24.

Chou, K. C., & Jiang, S. P. (1974) *Sci. Sin. 17*, 664–680.

Chou, K. C., & Zhou, G. P. (1982) *J. Am. Chem. Soc. 104*, 1409–1413.

Debyser, Z., Pauwels, R., Andries, K., Desmyter, J., Kukla, M., Janssen, P. A. J., & De-Clercq, E. (1991) *Proc. Natl. Acad. Sci. U.S.A. 88*, 1451–1455.

De-Clercq, E. (1987) *Antiviral Res. 7*, 1–10.

Deibel, M. R., McQuade, T. J., Brunner, D. P., & Tarpley, W. G. (1990) *AIDS Res. Human Retroviruses 6*, 329–340.

Dueweke, T. J., Kezdy, F. J., Waszak, G. A., Deibel, M. R., & Tarpley, G. W. (1991) *J. Biol. Chem. 267*, 27–30.

Gama Sosa, M., Fazely, F., Koch, J. A., Vercellotti, S. V., & Ruprecht, R. M. (1991) *Biochem. Biophys. Res. Commun. 174*, 489–496.

Goldman, M. E., Nunberg, J. H., O'Brien, J. A., Quintero, J. C., Schleif, W. A., Freund, K. F., Gaul, S. L., Saari, W. S., Wai, J. S., Hoffman, J. M., Anderson, P. S., Hupe, D., & Emini, E. A. (1991) *Proc. Natl. Acad. Sci. U.S.A. 88*, 6863–6867.

Lin, S. X., & Neet, K. E. (1990) *J. Biol. Chem. 265*, 9670–9675.

Majumbdar, C., Abbotts, J., Broder, S., & Wilson, S. H. (1988) *J. Biol. Chem. 263*, 15657–15665.

Merluzzi, V. J., Hargrave, K. D., Labadia, M., Grozinger, K., Skoog, M., Wu, J. C., Shih, C. K., Eckner, K., Hattox, S., Adams, J., Rosehthal, A. S., Faanes, R., Eckner, R., Koup, R. A., & Sullivan, J. L. (1990) *Science 250*, 1411–1413.

Moelling, K., Schulze, T., & Diringer, H. (1989) *J. Virol. 63*, 5489–5491.

Mohan, P., Singh, R., & Baba, M. (1991) *J. Med. Chem. 34*, 212–217.

Pauwels, R., Andries, K., Desmyter, J., Schols, D., Kukla, M. J., Breslin, H. J., Raeymaeckers, A., Van Gelder, J., Woestenborghs, R., Heykants, J., Schellekens, K., Janssen, M. A. C., De-Clercq, E., & Janssen, P. A. J. (1990) *Nature 343*, 470–474.

Reardon, J. E. (1992) *Biochemistry 31*, 4473–4479.

Romero, D. L., Busso, M., Tan, C. K., Reusser, F., Palmer, J. R., Poppe, S. M., Aristoff, P. A., Downey, K. M., So, A. G., Resnick, L., & Tarpley, W. G. (1991) *Proc. Natl. Acad. Sci. U.S.A. 88*, 8806–8810.

Schols, D., Pauwels, R., Desmyter, J., & De-Clercq, E. (1988) *Virology 175*, 556–561.

Tan, C. K., Zhang, J., Li, A. Y., Tarpley, W. G., Downey, K. M., & So, A. G. (1991) *Biochemistry 30*, 2651–2655.

Tramontano, E., & Cheng, Y. C. (1992) *Biochem. Pharmacol. 43*, 1371–1376.

Wu, J. C., Warren, T. C., Adams, J., Proudfoot, J., Skiles, J., Raghavan, P., Perry, C., Potocki, I., Farina, P. R., & Grob, P. M. (1991) *Biochemistry 30*, 2022–2026.